# SIMULATION OF WANDERING PHENOMENA IN BUBBLE PLUMES VIA A K-$\epsilon$ MODEL AND A LARGE-EDDY-SIMULATION (LES) APPROACH

**Fabián A. Bombardelli**[*], **Gustavo C. Buscaglia**[†]**, Marcelo H. García**[‡]**, and Enzo A. Dari**[†]

[*]Dept. of Civil and Environmental Engineering, University of California at Davis
Engineering III, One Shields Ave., Davis, CA 95616, USA
e-mail: fabombardelli@ucdavis.edu, web page: http://cee.engr.ucdavis.edu

[†]Centro Atómico Bariloche and Instituto Balseiro
Av. Bustillo Km. 9500, San Carlos de Bariloche, 8400 Río Negro, Argentina
e-mail: (gustavo)(darie)@cab.cnea.gov.ar, web page: http://www.cab.cnea.gov.ar

[‡]Ven Te Chow Hydrosystems Laboratory, Dept. of Civil and Environmental Engineering
University of Illinois at Urbana-Champaign
205 North Mathews Ave., Urbana, IL 61801, USA
e-mail: mhgarcia@uiuc.edu, web page: http://www.vtchl.uiuc.edu

**Key Words:** bubble plumes, plume wandering, k-$\epsilon$ model, Large-Eddy-Simulation approach, parallel computing.

**Abstract.** *In this paper, we focus on numerical simulations of the wandering phenomenon in bubble plumes, obtained with a new comprehensive model. The theoretical model has been developed from the theory of multi-component fluids. We have implemented that model in a finite-element, parallel platform.*

*After a brief discussion about the theoretical/numerical model, we describe and analyze the simulations of the wandering motion using the k-$\epsilon$ model. We show that this solution replicates wandering only for a relatively short period of time. The reasons for this fact are analyzed. Then, we present results obtained with the use of a Large-Eddy-Simulation (LES) approach. These results notably mimic observations of bubble plume wandering without any restriction.*

*Finally, we employ the unsteady results of the LES approach to perform a detailed analysis of turbulence in bubble plumes.*

## 1 INTRODUCTION

Multi-phase flows appear in numerous forms in Nature. They can be found in sediment-laden flows in rivers, in underflows associated with volcanic eruptions, in turbidity currents, in the bubbly wake of ships and in liquid-vapor mixtures in nuclear reactors, among many others. This article addresses basic aspects of the flow in a bubble plume, which is a simple paradigm of multiphase flow that appears in a many situations: They can be used as breakwaters, as destratification devices, and as containment for oil spills; they are also encountered in oil-well blowouts and in nuclear devices.

Although multiphase flows have been very well-known for long time, the theory to explain them is still under development. Mass, momentum, and energy equations for each of the phases are nowadays available. These equations are much more complex than their single-phase counterparts and they pose new challenges to their analytical and numerical treatment.

Several numerical solutions of the two-phase flow equations have been presented in the last decade. Still, the prediction capability of the models is not fully satisfactory, with the exception of a few cases. The advancement of computational power has not provided means to compensate the inherent theoretical difficulties of multi-phase flows.

The modeling of bubble plumes has received attention in the engineering community with special emphasis in the analysis of the flow in reactors and in ladles. The results typically show an acceptable prediction of time-averaged variables, but the analysis of turbulence is far from being well established. Very often, the description of turbulence in bubble plumes determines the difference between having a physically correct result, exceeding the issue of accuracy of the solution.

In this paper, we devote our efforts to the simulation and analysis of the phenomenon of wandering in bubble plumes. We focus on the numerical strategies for the replication of the wandering motion as well as the understanding of the interplay between eddies and bubbles during the quasi-period. The analysis include simulations in two and three dimensions.

## 2 THE WANDERING PHENOMENON. MODELING AND MEASUREMENTS

Plume wandering has received scientific attention for about fifty years now. It has been observed not only in bubble plumes but also in single-phase, thermal plumes.[1] It is believed to be a buoyancy-driven instability enhanced by the presence of walls. It is worth pointing out that the phenomenon has nothing to do either with a sort of "Magnus effect",[2] nor with "instabilities produced by excessive waves".[3]

Typically, the bubbles swarm from side to side in the three dimensional space in a random manner. The motion has a quasi-period that depends on the airflow rate of the plume, and the aspect ratio of the container. Delnoij *et al.*[4] found experimentally that the frequency of the wandering motion increases with the aspect ratio ($AR$) for a constant airflow rate up to a value of $AR \sim 4$, after which a constant value for the frequency is attained. Larger airflow rates produce *larger* frequency values, i.e., *smaller* periods. These trends were confirmed by Rensen and Roig.[5]

One set of measurements that has motivated much work during the last ten years is that performed by Becker et al..[6] Fig. 1 shows pictures of a bubble plume undergoing wandering in a box of 0.5 m of width, 1.5 m of water depth, and 0.08 m of thickness perpendicular to the paper. Becker et al. obtained velocity signals with Laser Doppler Anemometry (LDA), and presented time-averaged velocity fields.
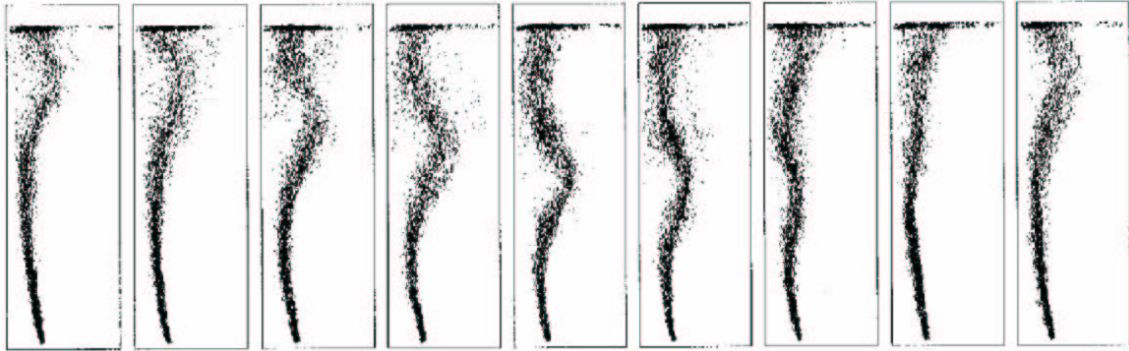


Figure 1: Wandering motion in a bubble plume. Experiments by Becker et al. (1994). Source: Sokolichin and Eigenberger (1999).

Other measurements associated with wandering, in containers of different size and shape, were presented by Mudde et al.,[7] Mudde and Van Den Akker,[8] Borchers et al.,[9] Becker et al.,[10] Lefebvre and Guy,[11] Pfleger et al.,[12] Rensen and Roig,[5] Brenn et al.,[13] and Buwa and Ranade.[14]

From the numerical point of view, the wandering phenomenon was the subject of several works, all of them employing finite differences. The state-of-the-art of the modeling of multi-phase flows is such that there is no ample consensus on basic issues. For instance, we can choose to perform an Eulerian description of the disperse phase, or a Lagrangean one. We could also adopt a full two-phase flow model or variants of it. In what follows, we review some of the previous works on the subject.

Tomiyama and Shimada[15] stated that only a multi-group modeling of bubble columns (i.e., including processes of break-up and coalescence) guarantees the replication of wandering, whereas Sokolichin and Eigenberger,[16] on the contrary, obtained wandering with a monodis-perse model. Several researchers have also employed complex models to reproduce wandering, all of them based on the two-fluid model (TFM). This means that there is still a debate on how to model wandering and that, following Loth,[17] the issue is still "what to model" rather than "how to model".

It is intuitive to think that the numerical scheme is crucial in allowing for the replication of wandering. Very diffusive schemes could preclude the motion altogether. Sokolichin et al.[18] showed that solutions obtained with a very simple model (and without any turbulence closure!) using both an "upwind" scheme and a second-order TVD scheme were able to simulate wander-ing. However, eddies in the upwind solution did not show the level of detail in the length scales of the TVD solution. Sokolichin et al. also concluded that Lagrangean and Eulerian approaches offer similar results, provided that a large number of particles is used (they suggested more than

100,000 particles). Later on, Sokolichin and Eigenberger[16] reproduced wandering again with a simple model and the k-$\epsilon$ turbulence closure. In turn, Deen *et al.*[19] could not obtain wandering with the k-$\epsilon$ closure, but they could with a LES approach. Mudde and Simonin, on the other hand,[20] stated that the addition of the lift force is mandatory to replicate wandering with the full TFM, a force that was not included in most of the previous (successful!) simulations.

This survey indicates that there are different alternatives to model two-phase flows in general and bubble plumes or columns in particular. No agreement or consensus has been attained.

Since the models developed in this work were implemented in a stabilized finite element platform, there is a clear question as to whether or not a stabilized-finite-element code can replicate wandering. We employ a quite simple two-fluid model with both RANS and LES turbulent closure, so as to address the effect of this closure on wandering prediction.

## 3 THEORETICAL AND NUMERICAL MODELS

In this section, we briefly review the theoretical and numerical models we developed in this work. We have presented more details in MECOM 2002 (see Buscaglia *et al.*, 2002[21]); in Buscaglia *et al.*;[22] Bombardelli, 2003;[23] Bombardelli *et al.*, 2003;[24] Bombardelli, 2004;[25] and Bombardelli *et al.*, 2004.[26]

### 3.1 Theoretical formulation

The equations of the TFM are obtained through ensemble averaging of the exact conservation equations for each phase in a multi-phase flow. According to Drew and Passman,[27] such model reads:

$$\frac{\partial \, \alpha_k \, \langle \rho_k \rangle}{\partial t} + div \, (\alpha_k \, \langle \rho_k \rangle \, \langle \vec{u_k} \rangle) \;\; = \;\; \Gamma_k \tag{1}$$

$$\frac{\partial \, \alpha_k \, \langle \rho_k \rangle \, \langle \vec{u_k} \rangle}{\partial t} + div \, (\alpha_k \, \langle \rho_k \rangle \, \langle \vec{u_k} \rangle \otimes \langle \vec{u_k} \rangle) \;\; = \;\; div \, \left[ \alpha_k \, \left( \langle T_k \rangle \, + \, T_k^{Re} \right) \right] +$$
$$+ \, \alpha_k \, \langle \rho_k \rangle \, \vec{b_k} + \vec{M_k} + \vec{v_{ki}}^{\,m} \, \Gamma_k \tag{2}$$

for the conservation equations of mass and momentum of the phases, respectively. (Notice that these are in fact four equations in an air-water mixture: two for each phase.) In (1) and (2), the subscript $k$ stands for $g$ in the case of the gaseous phase, and for $\ell$ in the liquid counterpart. The symbol $\langle \cdot \rangle$ is employed to denote the ensemble average operator, while $\alpha_k$ is the volume fraction of phase $k$; $\rho_k$ and $\vec{u_k}$ are the density, and the velocity vector of phase $k$. It is worth pointing out that the stress tensor indicated with the superscript $Re$ is the result of the process of ensemble averaging. The sum of both stress tensors is denoted by $T_k^* \;\; = \;\; \langle T_k \rangle \, + \, T_k^{Re}$. $\Gamma_k$ indicates the interfacial *mass transfer* source ($\sum_k \Gamma_k = 0$), and $\vec{v_{ki}}^{\,m} \, \Gamma_k$ expresses the interfacial *momentum* exchange due to *mass* transfer. $\vec{b_k}$ denotes the body force, $\vec{M_k}$ is the interfacial-force

and $\otimes$ refers to the tensor product. It can be shown that

$$\sum_k \left( \vec{v_{ki}}^m \, \Gamma_k \, + \, \vec{M_k} \right) \, = \, S\vec{T}F \tag{3}$$

where $S\vec{T}F$ represents the force coming from surface tension.

Our model defines *mixture* equations in terms of the velocity and density of the liquid and the gas.[22] In addition, certain non-linear terms are eliminated under the umbrella of the "dilute plume" hypothesis. These two steps allow for the recovery of a Navier-Stokes-equations structure for the mass and momentum conservation expressions (the forces in the momentum equations cancel out). Besides the ensemble average embedded in the TFM, either *time averaging* or *filtering* is formally necessary to account for turbulence. Time averaging is usually associated to RANS-type approaches; filtering is associated with Large-Eddy-Simulation (LES) approaches. Applying now the Reynolds' decomposition or the filtering, and denoting with the subscript $m$ the mixture variables, the final equations read:

$$\frac{\partial \rho_m}{\partial t} + div \left( \rho_m \, \overline{\vec{u_m}} \right) \; = \; 0 \tag{4}$$

$$\frac{\partial \rho_m \, \overline{\vec{u_m}}}{\partial t} + div \left( \rho_m \, \overline{\vec{u_m}} \otimes \overline{\vec{u_m}} \right) + \nabla \overline{p_m} \; = \; div \; (\sigma_m)_t - \rho_m \, g \, \mathbf{k} \tag{5}$$

where, $\overline{(\,\cdot\,)}$ indicates either Reynolds-averaging or filtering. The tensor $(\sigma_m)_t = -\rho_m \, \overline{u'_m \otimes u'_m}$ corresponds to Reynolds stresses in RANS and to residual stresses in LES.[28] Adopting a Newtonian model defining the mixture density

$$\rho_m \; = \; \rho_\ell \, \alpha_\ell \, + \, \rho_g \, \alpha_g \tag{6}$$

we obtain

$$div \, \overline{\vec{u_m}} \; = \; -\frac{1}{\rho^*} \left( \frac{\partial \rho^*}{\partial t} + \overline{\vec{u_m}} \cdot \nabla \rho^* \right) \tag{7}$$

$$\rho^* \frac{\partial \overline{\vec{u_m}}}{\partial t} + \rho^* \left( \overline{\vec{u_m}} \cdot \nabla \right) \overline{\vec{u_m}} + \nabla \hat{p}_m \; = \; div \left[ \mu_T \left( \nabla \overline{\vec{u_m}} + \nabla^T \overline{\vec{u_m}} \right) \right] - \rho_m g \, \mathbf{k} \tag{8}$$

where $\rho^*$ may be taken as $\rho_\ell$ (Boussinesq approximation) or as $\rho_m$; $\mu_T$ is the dynamic viscosity.

For the gaseous phase, our code includes several treatments of the mass and momentum equations.[24] The mass conservation equations result, with both ensemble and turbulent averaging:[22]

$$\frac{\partial}{\partial t} \overline{\langle C_O \rangle} + div \left( \overline{\langle C_O \rangle} \, \overline{\langle \vec{u_g} \rangle} \right) = \overline{S_O} + div \left( \frac{\mu_T}{\langle \rho_\ell \rangle \, Sc_g} \nabla \overline{\langle C_O \rangle} \right) \tag{9}$$

$$\frac{\partial}{\partial t} \overline{\langle C_N \rangle} + div \left( \overline{\langle C_N \rangle} \, \overline{\langle \vec{u_g} \rangle} \right) = \overline{S_N} + div \left( \frac{\mu_T}{\langle \rho_\ell \rangle \, Sc_g} \nabla \overline{\langle C_N \rangle} \right) \tag{10}$$

with $C_O$ and $C_N$ denoting the concentrations of gaseous oxygen and nitrogen, respectively, $S_O$ and $S_N$ indicating the mass transfer rates, and $S_{cg}$ referring to the Schmidt number.

In this paper we adopt an algebraic equation of the gas velocity:

$$\overline{\vec{u_g}} = \overline{\vec{u_\ell}} + w_b \, \mathbf{k} \tag{11}$$

where $w_b$ indicates the bubble-slip velocity. The model has been extended in the references given above so as to include a full momentum equation for the gas and the simulation of break-up and coalescence of bubbles.

## 3.2 Numerical treatment

The above equations were implemented in a parallel code based upon the finite element method. This code is a long-term development of Centro Atómico Bariloche, Argentina. Reports on successive stages of the code can be found in Buscaglia,[29] Lew,[30] Buscaglia *et al.*,[31] and Cantero.[32] Subroutines corresponding to the two-phase flow were coded at the Ven Te Chow Hydrosystems Laboratory, University of Illinois at Urbana-Champaign, in the context of the Ph.D. research of the first author. Details about the code can be found in Buscaglia *et al.*[22] and Bombardelli.[25]

In what follows, we will summarize some of the main features of the final implementation. The model employs an equal order formulation stabilized by pressure gradient projection, proposed by Codina and Blasco[33],[34] Several methods provide stability for the convective term: SUPG, SGS and GLS. In addition, diverse interpolation schemes are implemented.

In this paper, we have used bilinear quadrilateral elements in the 2D simulations, and linear tetrahedral elements in the 3D counterparts. The submodels associated with the turbulence treatment, the gaseous phases, and the liquid chemistry variables are advanced in time decomposing the time step into several substeps. The 3D cases were run in the IA-64 Linux Cluster at the National Center for Supercomputing Applications (NCSA) at Urbana-Champaign.

## 4 NUMERICAL RESULTS

Simulations in 2D and 3D, using diverse models, are reported. The simulations were carried out using a $k - \epsilon$ model and a LES approach, with the same airflow rate as in the experiments by Becker *et al.*,[6] corresponding to a superficial velocity of 1.6 mm/s. Whereas the first technique has been used in several papers, the application of LES *to this type of flow* has been scarce.[19],[35]

## 4.1 Simulations in two dimensions

Several papers[12],[16],[20] have shown that 2D simulations of the dynamic behavior of bubble columns lead to an overestimation of the eddy viscosity with a factor of about 5 to 10, as opposed to 3D simulations. Therefore, the transient character of the phenomenon is damped in the simulation, and the run is incapable of reproducing the wandering phenomenon. A steady-state is reached after some seconds. In 3D, overdiffusive numerical schemes could also overestimate the eddy diffusivity and thus dampen the 3D simulations as well.
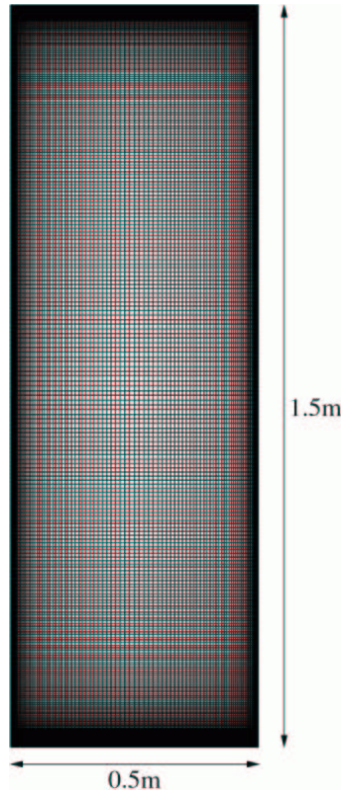
Figure 2: Fine mesh employed in the 2D computation of flow in a bubble column.

A quite extensive set of numerical tests, including variations in mesh, time step, stabilization techniques and closure models was undertaken to assess our model and numerical formulation.

Two 2D meshes were employed. The relatively "coarse" mesh contains 7,500 elements, with densification at the boundaries (50 x 150 in horizontal and vertical directions, respectively) and the fine mesh (Fig. 2) contains 30,000 elements (100 x 300). The "coarse" mesh corresponds to the finest grid employed by Sokolichin and Eigenberger in their 2D simulations.

The time step was varied between 0.1 and 0.0001 seconds. For the stabilization techniques, the SUPG and SGS were alternatively used. In most of the runs the *standard $k - \epsilon$* model was employed, as done by Sokolichin and Eigenberger,[16] Pfleger *et al.*,[12] and Buwa Ranade.[14] A constant value for the bubble-slip velocity equal to 0.2 m/s was initially used, but the algebraic model of Wüest *et al.* was also employed. The mass transfer has been supressed in the tests. Table 1 summarizes all the runs, which cover a different turbulent models, time and spatial steps, stabilization techniques and bubble-slip models.

*Despite the wide range of numerical and physical parameters varied during the tests, including the simulation of processes of break-up and coalescence, wandering could not be reproduced in the 2D simulations, i.e., a final steady-state condition was attained.* This result is in agreement with most of the previous tests found in the literature. As an illustration, Figure 3 shows the time series of a surrogate of the mean kinetic energy of the flow field, obtained as: $\int_{\Omega} 1/2 \, \rho_m \, u^2 \, d\Omega$, where $\Omega$ refers to the whole domain. It can be seen that a steady state

| Tests | D1 | D2 | D3 | D4 | D5 |
|---|---|---|---|---|---|
| Mesh | Coarse | Coarse | Fine | Fine | Fine |
| Model | Alg. | Alg. | Alg. | Alg. | Alg.. |
| Time step (sec.) | 0.1 | 0.01 | 0.1 | 0.01 | 0.1 |
| Stabil. technique | SUPG | SUPG | SUPG | SUPG | SGS |
| Rel. velocity | Ct=0.2 m/s | Ct=0.2 m/s | Ct=0.2 m/s | Ct=0.2 m/s | Ct=0.2 m/s |
| Size groups | NO | NO | NO | NO | NO |

| Tests | D6 | D7 | D8 | D9 |
|---|---|---|---|---|
| Mesh | Fine | Fine | Fine | Fine |
| Model | Alg. | Mom.-gas eqn. | Mom.-gas eqn. | Mom.-gas eqn. |
| Time step (sec.) | 0.0001 | 0.01 | 0.01 | 0.01 |
| Stabil. technique | SUPG | SUPG | SUPG | SUPG |
| Rel. velocity | Ct=0.2 m/s | Full | Full | Full |
| Size groups | NO | YES | YES | NO |

Table 1: Summary of 2D tests for the study of wandering effects in bubble columns.

is attained after the kinetic energy reaches a peak. Similar evolutions were obtained in all the cases tested.
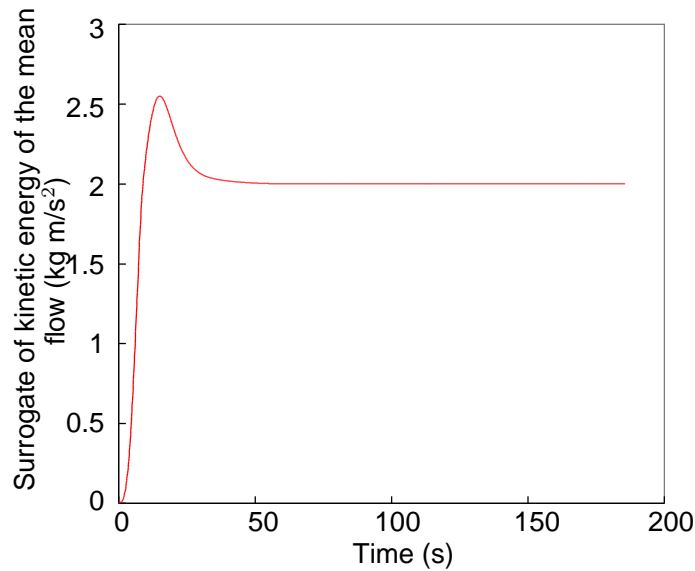


Figure 3: Time evolution of a surrogate of the kinetic energy of the flow in the 2D simulation of a bubble plume in a box.

Plots of the vertical velocity and turbulent kinetic energy fields for the steady-state situation (see Fig. 4) show qualitative agreement with the measurements.[16] Velocities are smaller than
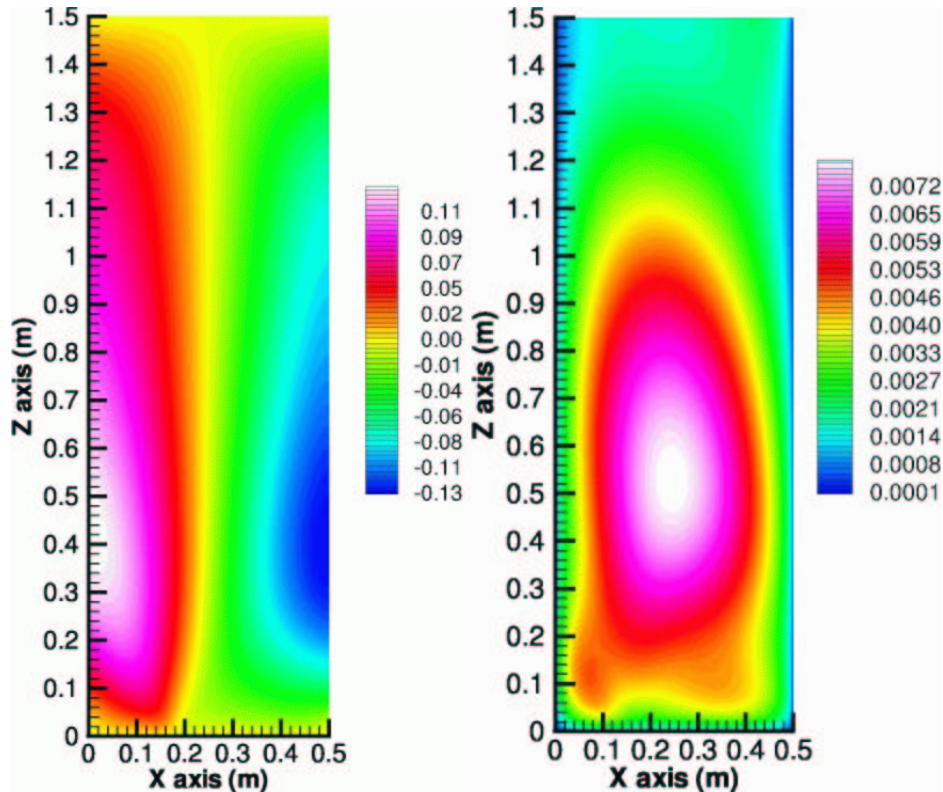
Figure 4: Vertical velocity (left) and turbulent kinetic energy (right) obtained in the 2D simulation of a bubble plume in a box. Values in m/s and m$^2$/s$^2$, respectively.

the measured ones due to excessive eddy viscosity (see Bombardelli 2004[25]). Notice that the maximum value of the turbulent kinetic energy is smaller than 0.01 m$^2$/s$^2$. Fig. 5 depicts the eddy viscosity obtained from these two-dimensional simulations. The average value of this variable is 3 x 10$^{-3}$ m$^2$/s.

Similar results were obtained in the simulations performed with other combinations of the above variables. All the runs attained a final steady-state condition.

The conclusion of this section is that *none* of the investigated models and schemes (which cover some alternatives not considered in the literature) reproduces in 2D the spontaneous quasi-periodic behavior identified in the experiments.

## 4.2 Simulations in three dimensions

The runs in three dimensiions were performed first with the $k - \epsilon$ model and, then, with the LES treatment. Table 2 summarizes those runs undertaken with three-dimensional setups.
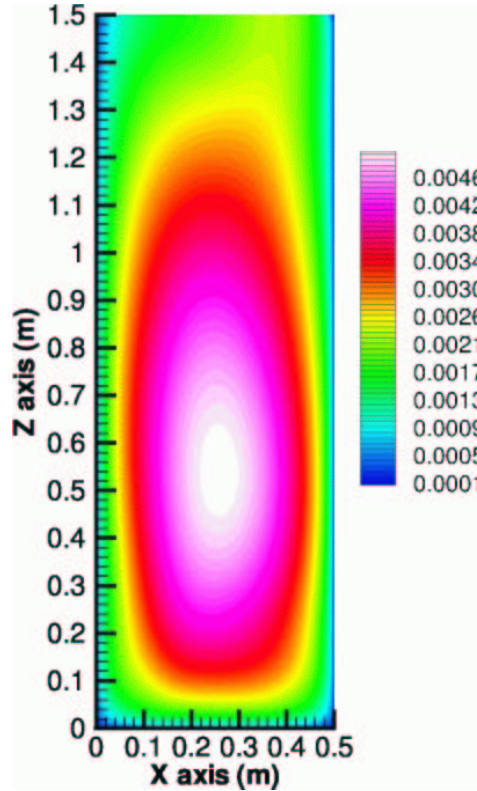
Figure 5: Eddy viscosity obtained in the 2D simulation of a bubble plume in a box. Values in m$^2$/s.

| Tests | D10 | D11 | D12 | D13 | D14 |
|---|---|---|---|---|---|
| Mesh | Coarse | Coarse | Fine | Fine | Fine |
| Model | Alg. | Alg. | Alg. | Alg. | Alg. |
| Time step (sec.) | 0.1 | 0.01 | 0.1 | 0.01 | 0.1 |
| Stabil. technique | SUPG | SUPG | SUPG | SUPG | SGS |
| Rel. velocity | Ct=0.2 m/s | Ct=0.2 m/s | Ct=0.2 m/s | Ct=0.2 m/s | Ct=0.2 m/s |
| Turb. model | k-e | k-e | k-e | k-e | LES |

Table 2: Summary of 3D tests for the study of wandering effects in bubble columns.

### 4.2.1  Runs with the $k - \epsilon$ model

A uniform mesh size of 0.01 m (50 x 150 x 8) was adopted, with a time step equal to 0.1 sec. This choice is supported by published results.[16] This is the mesh termed as "coarse" in Table 2. The initial conditions were set at rest. Regarding the boundary conditions, wall functions were used in five faces of the box, whereas a symmetry condition was employed for the free surface. The runs took about 12 hours to simulate 60 seconds in 5 processors of the Linux Cluster at NCSA, and were extended for about 1000 s.

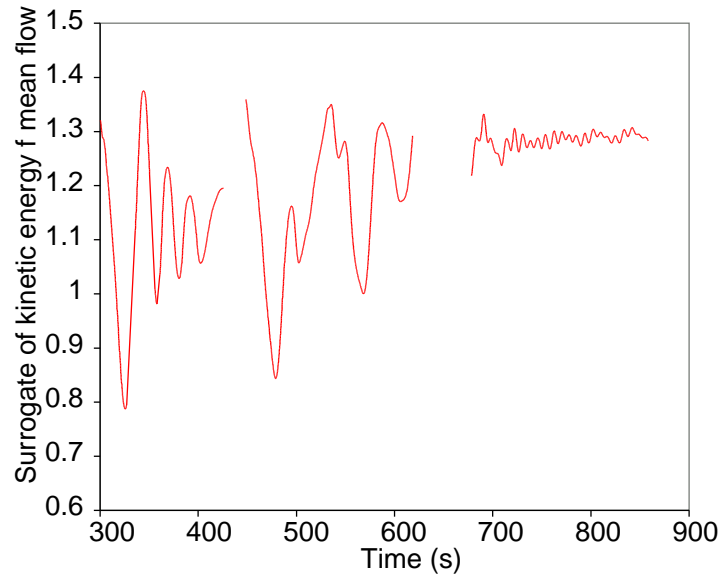Fig. 6 depicts the time evolution of a surrogate of the kinetic energy of the mean flow, for run

Figure 6: Time evolution of a surrogate of the kinetic energy of the flow in the 3D simulation of a bubble plume in a box. $k - \epsilon$ model. Three segments of the time evolution are displayed.

D10. Three segments of the time evolution are shown. A quasi-periodic motion develops at the beginning of the simulation (approximately, first 500 s) but then *the wandering motion disappears*. The first part is consistent with Sokolichin and Eigenberger's results, but the suppression of motion is consistent with the findings of other authors.[19] It becomes obvious that performing the simulation for short times may have hidden in some works the steady-state that settles later on. Fig. 7 shows snapshots of gaseous oxygen concentration (which is a good surrogate for bubble density) on the mid-thickness plane for different times obtained in run D10, showing the unsteady behavior in the first part of the simulation. Larger values are displayed in yellow and red, whereas smaller values are presented in blue. Notice that the resemblance with Fig. 1.

Fig. 8 shows contours of *velocity magnitude* of the mixture. Again, largest values are presented in yellow. Each of the "rings" is a vortex that interplays with other vortices and with the walls. As anticipated by Sokolichin and Eigenberger it is possible to notice that the "initial" single vortex bifurcates into two, and then into three smaller vortices, as a result of the motion of the plume. Later, two vortices appear again via the combination of two and, finally, one vortex dominates the box again. This number of vortices naturally depends upon the width/water depth ratio, as demonstrated by Delnoij *et al.*[4] and Borchers *et al.*[9] This description of the flow agrees completely with Sokolichin and Eigenberger's counterpart. From the values of dissipation rate, Kolmogorov length scales have been obtained in all the domain, ranging from 0.1 mm to more than 3 mm. Most of the Kolmogorov length scales ranged from 0.1 to 1 mm.
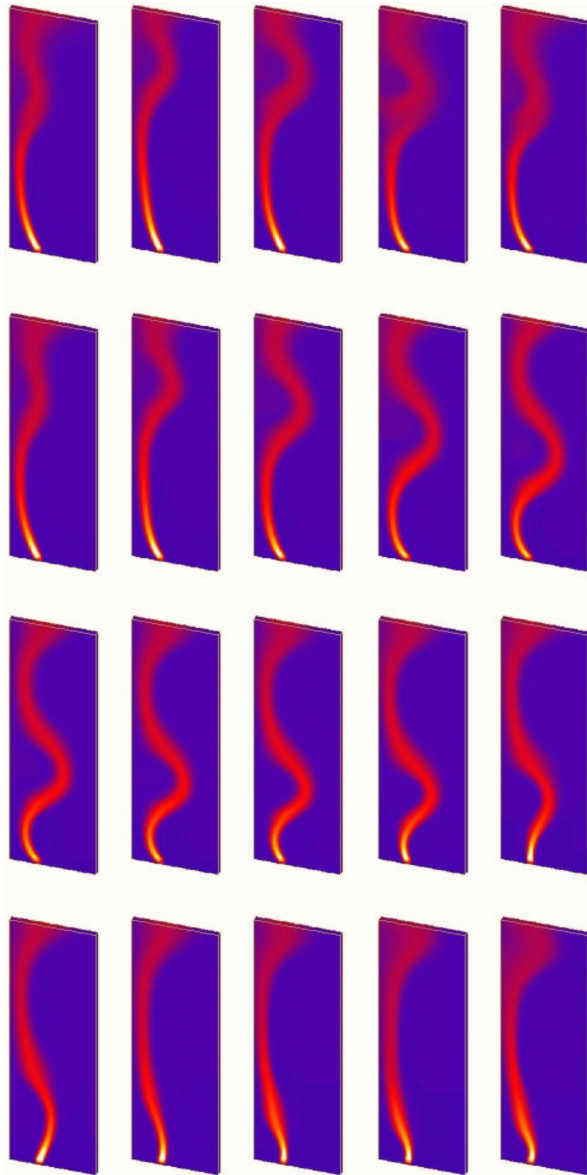
1979

Figure 7: Snapshots of oxygen concentration in the 3D simulation of a bubble plume in a box. $k - \epsilon$ model.

### 4.2.2 Results corresponding to the run with the LES approach

In the LES computations, 2,870,400 elements were employed, corresponding to a uniform mesh size of 5 mm and to a mesh of 300 x 100 x 16. This mesh size is two times smaller than Deen *et al.*'s.[19] It is also about 5 to 10 times the Kolmogorov length scale computed from the $k - \epsilon$ run. The time step was fixed at 0.1 s, which is consistent with the Courant number of 1 suggested by Piomelli.[36] The effect of a smaller time step of 0.01 s was also investigated once the quasi-periodic behavior had been attained (run D11, see below).

One important question is whether there is a need for a modification of the Smagorinsky's
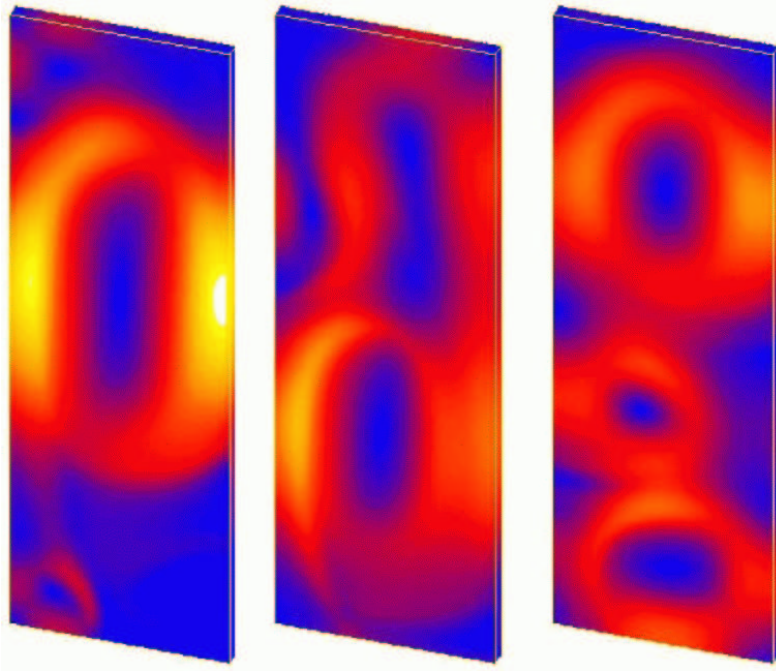
Figure 8: Snapshots of velocity magnitude in the 3D simulation of a bubble plume in a box. $k - \epsilon$ model. The images are not separated the same amount of seconds.

model when a disperse phase is present. In our runs we adopt the standard Smagorinsky's model to address this issue.

Based on the experience with the $k - \epsilon$ model in the previous runs, it was decided to test a couple of *different initial conditions* and to run those tests for a very long time. It was concluded that after 80 s (about two periods of the wandering motion), the run was practically independent of the initial conditions. Fig. 9 shows the time evolution of a surrogate of the kinetic energy of the mean flow. It is possible to see that, in fact, a quasi period of basically 50 s characterizes the motion after 75 s. However, larger quasi periods are also found. For instance, considering the curve close to 260 s, the quasi period therein is about 80 s.

Regarding the boundary conditions, the airflow rate was imposed in a volume located from 0.15 to 0.19 m from the left wall. The velocity vectors at different planes not so close to the diffuser were found insensitive to this exact location. The gas flow rate was kept constant during all the computations, not including any random component. The velocity boundary conditions at the walls were set enforcing the law of the wall. This approach is called LES-NWM,[28] i.e., a LES with near-wall modeling. The runs required 7 hours for every 9 seconds of simulation on 20 processors of the Linux Cluster at NCSA.

Fig. 10 depicts snapshots of the contours of gaseous oxygen concentration for the case of the simulation with LES, separated by 0.5 s. Some small length scales can be observed in the plume, giving information about details of its behavior in diverse parts of the box. In turn, Fig. 11 presents snapshots of gaseous oxygen concentration separated by 5.5 s, comprising a quasi period of the dynamic motion. The numerically-predicted quasi period was slightly larger than
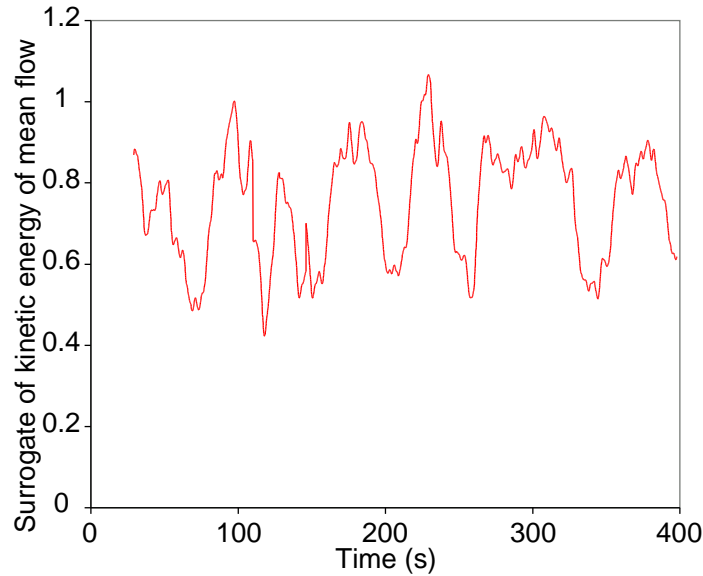
Figure 9: Time evolution of a surrogate of the kinetic energy of the flow in the 3D simulation of a bubble plume in a box. LES approach.

the measured value of 41 seconds. *It can be noticed that the simulation satisfactorily mimics the measurements.*

Fig. 12 presents the velocity fields of the mixture corresponding exactly to the above oxygen concentrations. Notice that, as expected, the large coherent structures that were apparent in the $k - \epsilon$ model solution appear in the LES counterpart, but embedded in a large spectrum of smaller scales. These smaller scales are characterized in the following sections.

Compared to the simulations undertaken with the $k - \epsilon$ model, the LES results give a vivid picture of the features of the instability associated to wandering. It is possible to see from Figs. 10 to 12 that the bubble plume, laden towards the left wall, follows regions of relatively high velocity of the carrier, with exception of the upper part of the box. In that region, the plume oscillates back and forth with respect to the wall in the first stages of the quasi period. This oscillation is produced by the Coanda effect.[37] The motion is the source of a vortex on the top-left corner, at the beginning of the quasi period (see Fig. 13, section (a)). This eddy keeps its size for later times, interacting with the large vortex located in the rest of the box. At the same time, it is convected downwards by the mean flow. This eddy diminishes the size of the eddy occupying the remaining of the box, leading to the condition of two vortices (section (b)). The eddy coming from the upper-left corner continues in its way down until an eddy forms in the top-right corner of the box (section (c)). This leads to the three-vortex situation. This condition lasts until the two lower eddies "merge," restoring a two-vortex condition (section (d)). Finally, a single vortex is left in lieu of the two vortices (section (e)).
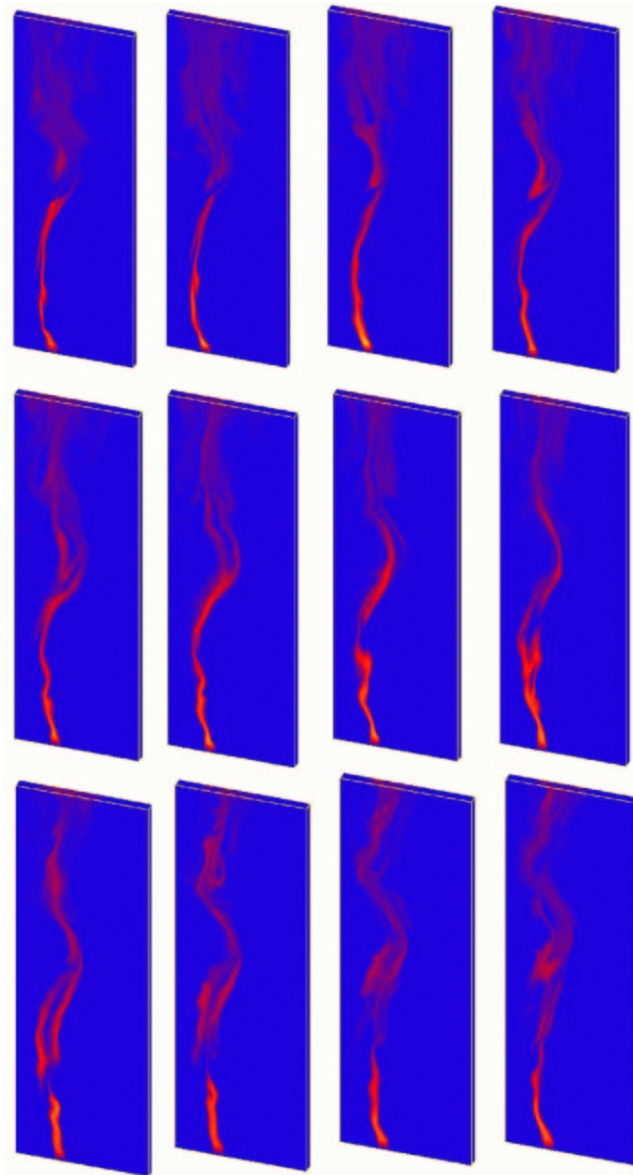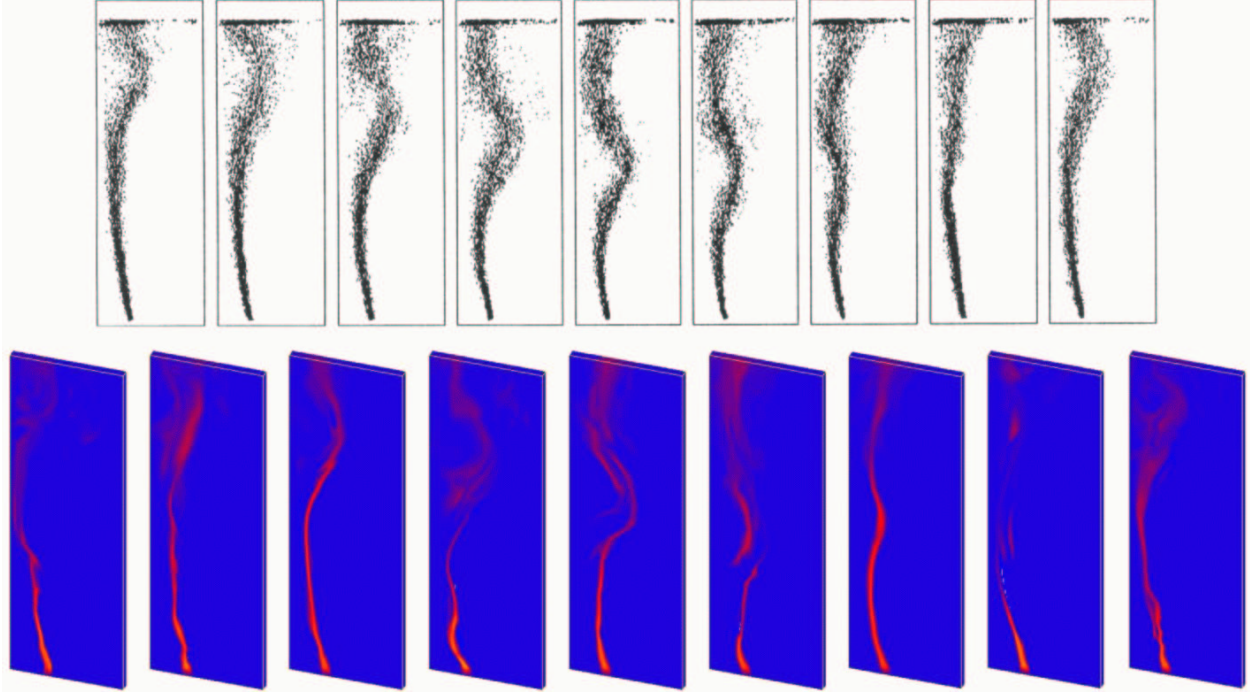
Figure 10: Evolution in time of the oxygen concentration in the 3D simulation of a bubble plume in a box. The images are separated by 0.5 seconds. LES approach.

## 5   ANALYSIS OF TURBULENCE FROM 3D SIMULATIONS

The availability of "instantaneous" velocity fields from the LES computations allowed for the determination of turbulence statistics. The 3D outputs from the numerical solution were post-processed in order to obtain statistical moments up to fourth order, turbulent kinetic energy, turbulent shear stresses and the structure of the flow. This also allowed for the characterization of the coherent structures induced by the wandering motion.

Figure 11: Evolution in time of the oxygen concentration in a quasi period of in the 3D simulation of a bubble plume in a box. The images are separated by 5.5 seconds. LES approach.

## 5.1 Turbulence statistics

For the different statistical moments, the usual definitions were applied at each node of the mesh:[38]

$$U_i = \overline{u}_i \equiv \frac{1}{NF} \sum_{j=1}^{NF} u_{i,j} \; ; \qquad \sigma_i^2 \equiv \frac{1}{(NF-1)} \sum_{j=1}^{NF} [u_{i,j} - \overline{u}_i]^2 \; ;$$

$$S_i \equiv \frac{1}{(NF-1)\,s^3} \sum_{j=1}^{NF} [u_{i,j} - \overline{u}_i]^3 \; ; \qquad K_i \equiv \frac{1}{(NF-1)\,s^4} \sum_{j=1}^{NF} [u_{i,j} - \overline{u}_i]^4 \quad (12)$$

where $u$ represents any of the velocity components, $i$ refers to the node in the mesh, $j$ indicates time, and $s$ is the standard deviation. The overbar means time average, whereas $NF$ is the number of files (values) that were used in the computations. The above equations correspond to the time average, variance, skewness and kurtosis, respectively. From the variances for the three velocity components, the turbulent kinetic energy was obtained at each point. The estimator of the variance above is a non-biased estimator.[38] Additionally, the nondimensional turbulent stress was computed from:

$$\left( \frac{\overline{u_k' u_l'}}{U_k U_l} \right)_i = \frac{1}{NF} \frac{\sum_{j=1}^{NF} [u_{k_{i,j}} - \overline{u}_{ki}][u_{l_{i,j}} - \overline{u}_{li}]}{\overline{u}_{ki}\,\overline{u}_{li}} \qquad no\ summation\ implied \quad (13)$$
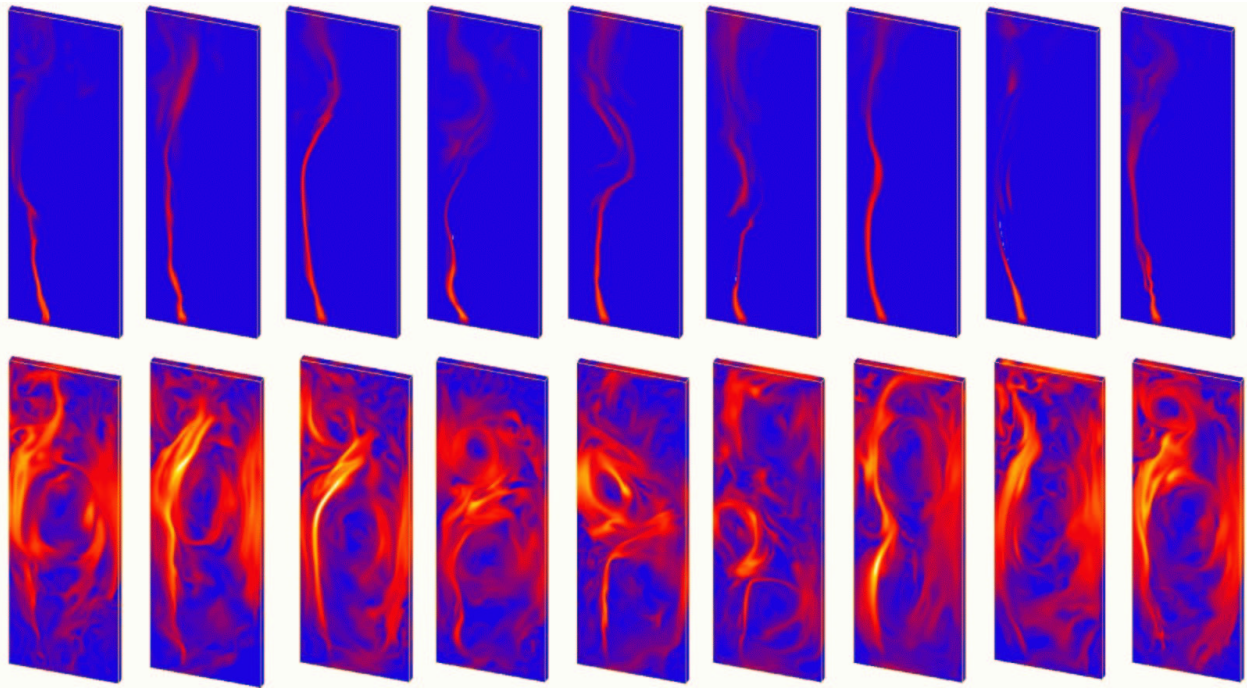
Figure 12: Evolution in time of the velocity magnitude in a quasi period of in the 3D simulation of a bubble plume in a box. The images are separated by 5.5 seconds. LES approach. Notice the correspondence with some images of Figure 8.
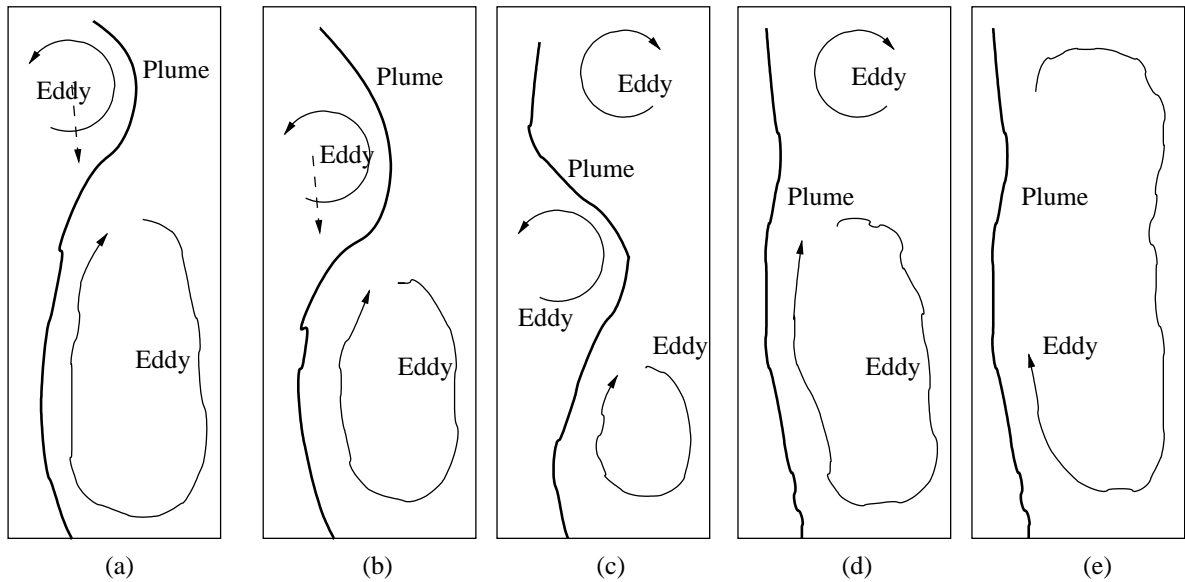


Figure 13: Sketch of the evolution of the number of eddies and their interrelation with the bubble plume.

where $i$ and $j$ are as above and $k$ and $l$ indicate the velocity components.

Computations were undertaken using different numbers of files, to address the issue of sta-

tionarity of the statistics. The smallest number of files was 487, which covered 225 seconds of simulation, 5.5 quasi periods of plume wandering. It was confirmed that the statistics were indeed stationary when 250 s were processed, with the exception of the third moment. This processing took about 2 hours of computer time.

Fig. 14 brings a comparison between the present numerical results and the measurements provided by Sokolichin and Eigenberger.[16] Time-averaged vertical velocities, at different heights above the diffuser, for the plane located at mid-thickness, are compared. The agreement is very satisfactory, considering both the short period of time-averaging of the measurements (between 30 and 60 s), and the nature of the model. There are some discrepancies close to the diffuser that could be attributed to the inexact boundary condition. Fig. 15 in turn shows projected vectors of the time-averaged velocity field obtained with the LES approach. Planes are parallel to the front wall and are located at 2, 4, 5.5 and 7 cm from the front wall. The color of vectors indicate the value of the vertical velocity. Notice that the patterns are quite similar in all the planes, which confirms the essentially-2D nature of the flow.

Fig. 16 presents the TKE at mid-thickness computed from the LES results. Compared to Figure 4(b), it is seen that the computed values with LES present a peak on the left which is more than two times larger than the 2D results. This result can be explained clearly as follows. TKE can be interpreted roughly as a surrogate of the velocity fluctuations. The 3D simulations include wandering and, thus, a portion of the fluctuations is associated with the motion of the plume, and *not* with "true" turbulence. Consequently, the wandering kinetic energy, not necessarily *turbulent* kinetic energy, is accounted for in the plot. In order to obtain the true TKE, a high-pass filter is needed, as employed by Mudde *et al.*[7]

Fig. 17 investigates the distribution of variance of the velocity components in the vertical direction, for planes located at 4, 5.5, and 7 cm from the front face of the box. It is clearly seen that the variance increases with distance from the diffuser up to a certain elevation, and then it saturates, as reported by Rensen and Roig,[5] for both velocity components. This was attributed by Rensen and Roig to the effect of the walls. However, whereas the horizontal velocity component seems to show a saturation in the upper 60% of the box, the vertical component of the velocity vector shows a decreasing value in the upper 50 cm, close to the left wall. This difference could be the result of the fact of having a non-symmetric plume. Closer to the right wall, the pattern is similar to that corresponding to the horizontal velocity component. These results are subjected to the same issues corresponding to the TKE, in terms of the superposition of wandering motion and true turbulence.

Fig. 18 shows the kurtosis of the velocity components in the vertical direction, at planes located at 4, 5.5, and 7 cm from the front wall. Kurtosis is a measure of the "non-gaussianity" of the distribution. For a Gaussian distribution the value of the kurtosis is 3. Notice from the figure that the vertical velocity presents values greater than 3. The horizontal component has values close to 3. Similar issues associated with the superposition of wandering motion and true turbulence appear in these figures. Overall, the LES results are consistent with the physics and with the measurements.
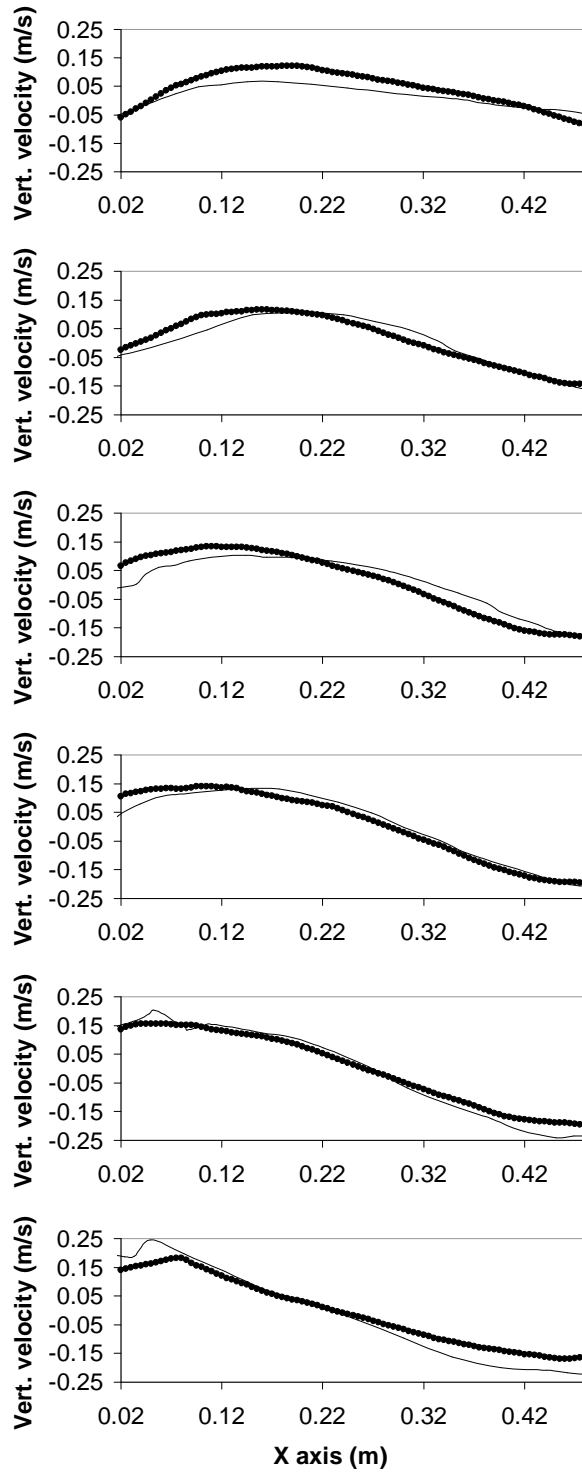
Figure 14: Comparison of modeled and measured vertical velocities at different planes above the diffuser, for the 3D simulation of a bubble plume in a box. LES approach. Numerically-obtained values are represented by dots, showing the fine resolution; measurements are represented by solid lines. Planes correspond to (from top to bottom): 1.44, 1.25, 1.06, 0.86, 0.67, and 0.48 m above the bottom of the tank.
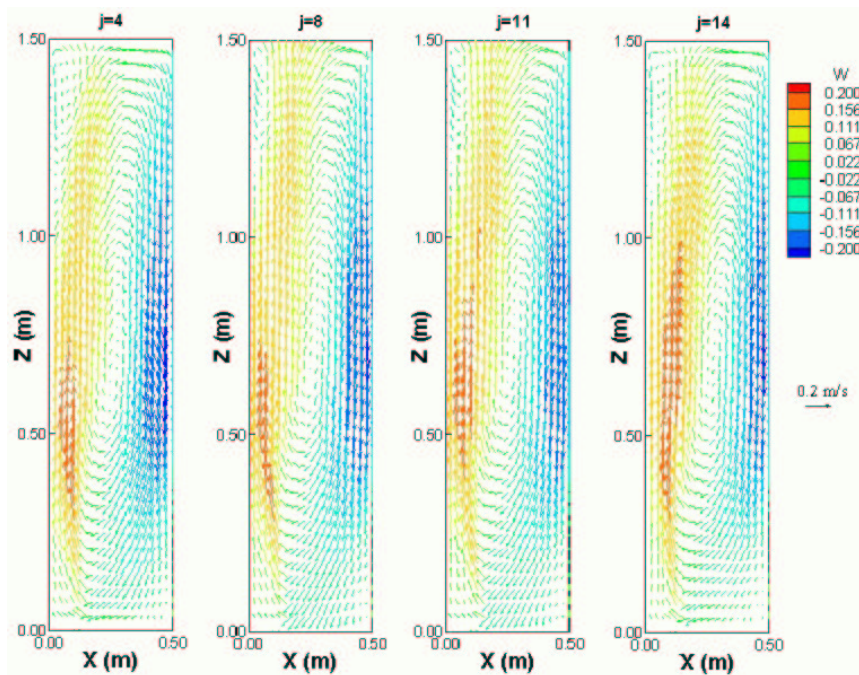
Figure 15: Velocity fields for different planes parallel to the front wall. Planes are located at 2, 4, 5.5, and 7 cm from the front wall. Colors of the vectors indicate the value of the vertical velocity.
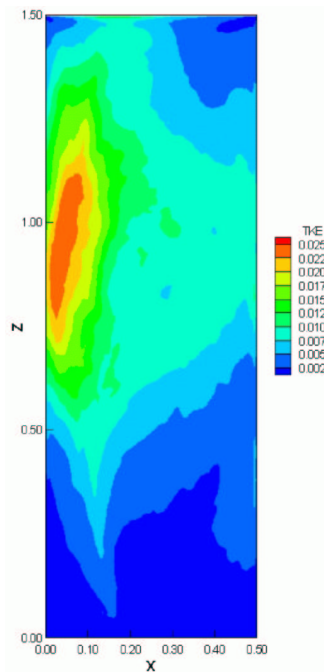


Figure 16: Distribution of turbulent kinetic energy in a plane located at mid-thickness. Values are expressed in m$^2$/s$^2$.
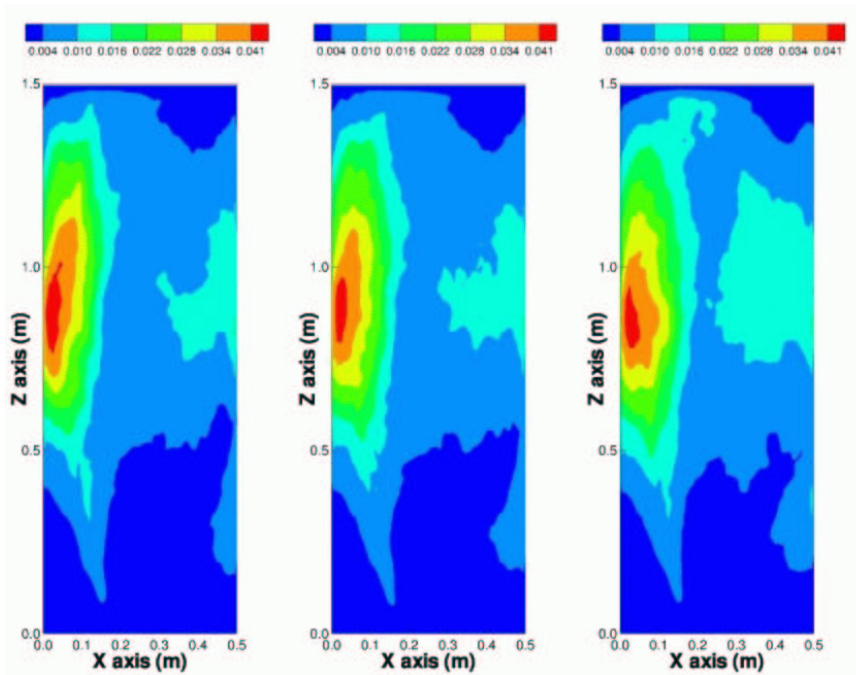
Figure 17: Distribution of the variance of the velocity component in the vertical direction. Planes located at 4, 5.5, and 7 cm from the fron face of the box.
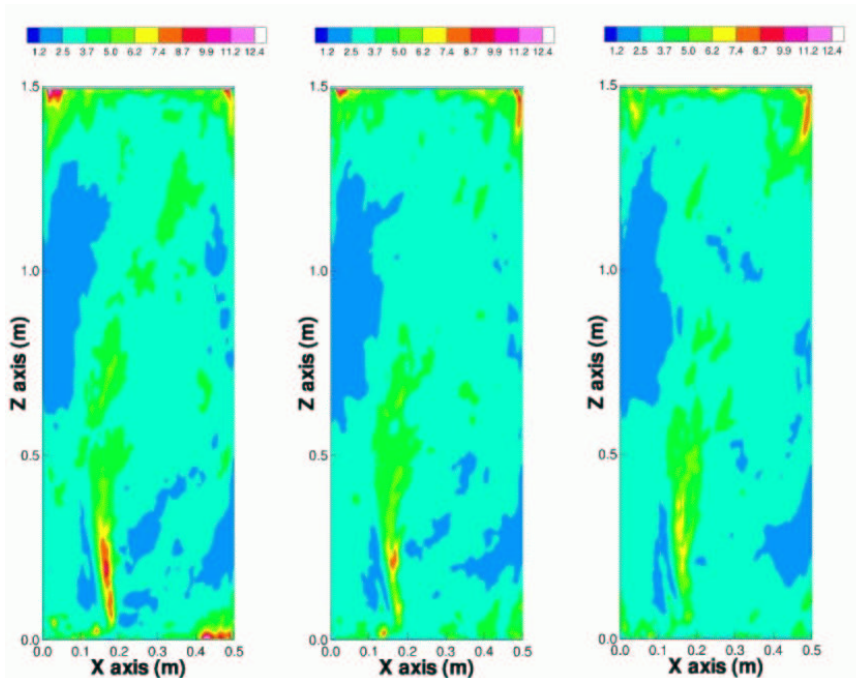


Figure 18: Distribution of the kurtosis of the velocity component in the vertical direction. Planes located at 4, 5.5, and 7 cm from the fron face of the box.

## 5.2 Characterization of coherent structures of the flow produced by the wandering motion

Although turbulent flows are intrinsically random, some of them show certain scales that can be characterized according to their persistent structure. These scales are called "coherent structures".[39] In the phenomenon of wandering, and with the configuration of a box, there appear eddies which interact with each other, with the walls, and with the bubbles. The eddies persist for some time, then dissapear and appear again in the next quasi-period. These eddies are the coherent structures associated with the wandering motion. In order to characterize those structures, several analyses have been developed.
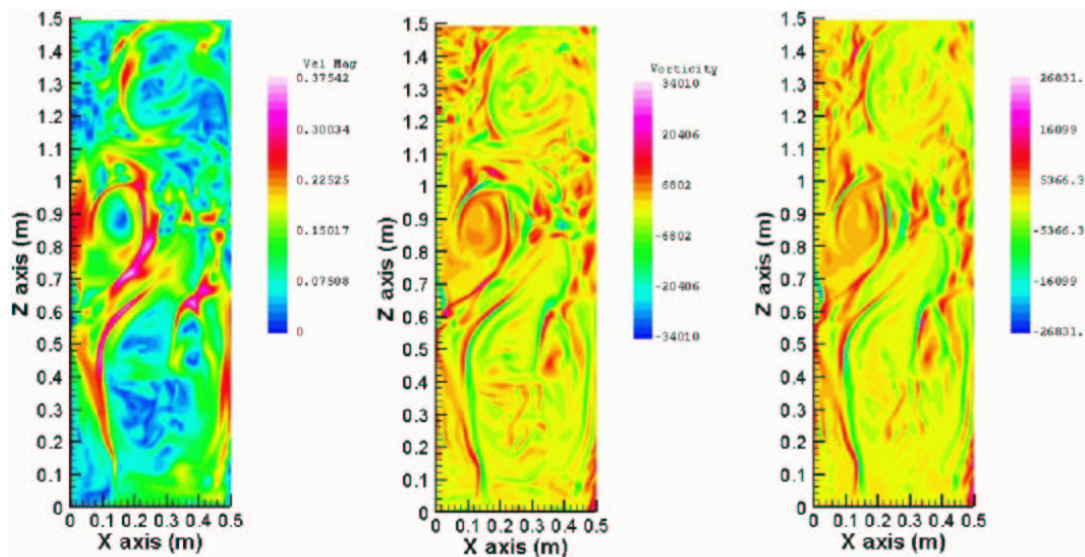


Figure 19: Two-dimensional velocity, vorticity and velocity gradients in a plane located at 4 cm (mid-thickness) from the front wall of the box. The values of vorticity and velocity gradients are multiplied by $10^3$.

Fig. 19 shows the contours of:

- the two-dimensional instantaneous velocity (in m/s),

- the instantaneous "y"-vorticity component (in 1/s, multiplied by $10^3$), and

- the instantaneous horizontal gradient of vertical velocity ($\partial w/\partial x$, in 1/s, also multiplied by $10^3$),

corresponding to a two-vortex condition in the box, for a plane located at mid-thickness (4 cm). The horizontal gradient of "$u_z$" completely dominates the vorticity component field. The plane located at 4 cm presents a wide range of scales, that are not present closer to the walls. Additionally, it is possible to see that bubbles do not tend to be trapped by the eddies. Sene et al.[40] determined in a mixing layer that 50% of the bubbles are trapped if $\Gamma_{SHT} = \Delta U/v_{term}$, the "trapping parameter", is about 3. This parameter measures the tendency for a bubble to

be trapped through $\Delta U$, the velocity difference across the vortex. In this case, this ratio is about 1, which means that bubbles are not trapped. Finally, the interplay among eddies and bubbles resembles Wang and Maxey's[41] sketch of the preferential sweeping mechanism for heavy particles interacting with vortical structures.

## 6 CONCLUSIONS

Intensive computations regarding bubble plume wandering have been presented. They have shown that it is possible to reproduce wandering effects with our finite element model in 3D. This could be achieved with a LES approach with a very simple bubble-slip model and Smagorinsky's subgrid closure.

With the $k - \epsilon$ model, on the other hand, short simulation times do show wandering, but at longer times the flow settles to a steady state.

The quasi-period (the motion is not strictly periodic) of the wandering predicted by the simulation was found to agree reasonably well with the measured one. The agreement between the modeled and observed position of the plume was very satisfactory. The coherent structures that take place in the interplay between eddies and bubbles have been characterized using vorticity fields. It has been shown that bubbles are not trapped by the eddies.

## REFERENCES

[1] K. Kotsovinos. Plane turbulent buoyant jets. Part 2. Turbulence structure. *J. Fluid Mech.*, **81-1**, 45–62 (1977).

[2] S. Johansen, D. Robertson, K. Wohe, and T. Engh. Fluid dynamics in bubble stirred ladles: Part I. Experiments. *Metall. Trans. B*, **19B**, 745–754 (1988).

[3] A. Castillejos and J. Brimacombe. Measurement of physical characteristics of bubbles in gas-liquid plumes: Part II. Local properties of turbulent air-water plumes in vertically injected jets. *Metall. Trans. B*, **18B**, 659–671 (1987).

[4] E. Delnoij, J. Kuipers, and W. van Swaaij. Dynamic simulation of dispersed gas-liquid two-phase flow: Effect of column aspect ratio on the flow structure. *Chem. Eng. Sci.*, **52**, 3759–3772 (1997).

[5] J. Rensen and V. Roig. Experimental study of the unsteady structure of a confined bubble plume. *Int. J. Multiphase Flow*, **27**, 1431–1449 (2001).

[6] S. Becker, A. Sokolichin, and G. Eigenberger. Gas-liquid flow in bubble columns and loop reactors: Part II. Comparison of detailed experiments and flow simulations. *Chem. Eng. Sci.*, **49**, 5747–5762 (1994).

[7] R. Mudde, J. Groen, and H. Van Den Akker. Liquid velocity field in a bubble column: LDA experiments. *Chem. Eng. Sci.*, **52**(21-22), 4217–4224 (1999).

[8] R. Mudde and H. Van Den Akker. Dynamic behavior of the flow field of a bubble column at low to moderate gas fractions. *Chem. Eng. Sci.*, **54**, 4921–4927 (1999).

[9] O. Borchers, C. Busch, A. Sokolichin, and G. Eigenberger. Applicability of the standard $k - \epsilon$ turbulence model to the dynamic simulation of bubble columns: Part II. Comparison of detailed experiments and flow simulations. *Chem. Eng. Sci.*, **54**, 5927–5935 (1999).

[10] S. Becker, H. De Bie, and J. Sweeney. Dynamic flow behaviour in bubble columns. *Chem. Eng. Sci.*, **54**, 4929–4935 (1999).

[11] S. Lefebvre and C. Guy. Characterization of bubble column hydrodynamics with local measurements. *Chem. Eng. Sci.*, **54**, 4895–4902 (1999).

[12] D. Pfleger, S. Gomes, N. Gilbert, and H. Wagner. Hydrodynamic simulations of laboratory scale bubble columns fundamental studies of the Eulerian-Eulerian modeling approach. *Chem. Eng. Sci.*, **54**, 5091–5099 (1999).

[13] G. Brenn, H. Braeske, and F. Durst. Investigation of the unsteady two-phase flow with small bubbles in a model bubble column using phase-Doppler anemomentry. *Chem. Eng. Sci.*, **57**, 5143–5159 (2002).

[14] V. Buwa and V. Ranade. Dynamics of gas-liquid flow in a rectangular bubble column: Experiments and single/multi-group CFD simulations. *Chem. Eng. Sci.*, **57**, 4715–4736 (2002).

[15] A. Tomiyama and N. Shimada. A numerical method for bubbly flow simulation based on a multi-fluid model. *J. Pressure Vessel Technology*, **123**, 510–516 (2001).

[16] A. Sokolichin and G. Eigenberger. Applicability of the standard $k - \epsilon$ turbulence model to the dynamic simulation of bubble columns: Part I. Detailed numerical simulations. *Chem. Eng. Sci.*, **54**, 2273–2284 (1999).

[17] E. Loth. Numerical approaches for motion of dispersed particles, droplets and bubbles. *Progress in Energy and Combustion Sci.*, **26**, 161–223 (2000).

[18] A. Sokolichin, G. Eigenberger, A. Lapin, and A. Lübert. Dynamic numerical simulation of gas-liquid two-phase flows. Euler/Euler versus Euler/Lagrange. *Chem. Eng. Sci.*, **52**, 611–6626 (1997).

[19] N. G. Deen, T. Solberg, and B. Hjertager. Large eddy simulation of the gas-liquid flow in a square cross-sectioned bubble column. *Chem. Eng. Sci.*, **56**, 6341–6349 (2001).

[20] R. Mudde and O. Simonin. Two- and three-dimensional simulations of a bubble plume using a two-fluid model. *Chem. Eng. Sci.*, **54**, 5061–5069 (1999).

[21] G. Buscaglia, E. Dari, F. Bombardelli, and M. García. Numerical modeling of flow and mass transfer in bubble plumes. *Mecánica Computacional, Proceedings MECOM'2002*,

**21**, 541–565 (2002).

[22] G. Buscaglia, F. Bombardelli, and M. García. Numerical modeling of large-scale bubble plumes accounting for mass transfer effects. *Int. J. Multiphase Flow*, **28**, 1763–1785 (2002).

[23] F. Bombardelli. Characterization of coherent structures from parallel, LES computations of wandering effects in bubble plumes. In P. Bizier and P. DeBarry, editors, *Proc. World Water and Environmental Resources Congress, Philadelphia, USA*. ASCE-EWRI, (2003).

[24] F. Bombardelli, G. Buscaglia, and M. García. Parallel computations of the dynamic behavior of bubble plumes. In F. W. Brust, editor, *Proc. Pressure Vessels and Pipe Division Conference, Cleveland*, volume PVP-464, Residual Stress, Fitness-For-Service, and Manufacturing Processes. ASME-PVP Division, (2003).

[25] F. Bombardelli. *Turbulence in multiphase models for aeration bubble plumes*. PhD thesis, University of Illinois at Urbana-Champaign, Department of Civil and Environmental Engineering, (2004).

[26] F. Bombardelli, G. Buscaglia, and M. García. Theoretical and numerical models for aeration bubble plumes, including processes of break-up and coalescence. in preparation.

[27] D. Drew and S. Passman. *Theory of Multicomponent Fluids*, volume 135 of *Applied Mathematical Sciences*. Springer, (1999).

[28] S. Pope. *Turbulent flows*. Cambridge University Press, (2000).

[29] G. Buscaglia. GPFEP. A system for the generation of finite element programs. Technical report, Centro Atómico Bariloche, Bariloche, Argentina, (1995). (In Spanish).

[30] A. Lew. The finite element method in high-performance computing environments. Master thesis, Instituto Balseiro, Bariloche, Argentina, (1997). In Spanish.

[31] G. C. Buscaglia, E. A. Dari, A. J. Lew, and M. Raschi. Un programa general de elementos finitos en paralelo. In C. García Garino et al, editor, *Proceedings VI Congreso Argentino de Mecánica Computacional (Mendoza)*, pages CD–ROM. Ex-Libris, (1999).

[32] M. Cantero. Simulation of thermally-coupled turbulent flows with obstructions. Master thesis, Instituto Balseiro, Bariloche, Argentina, (2000). (In Spanish).

[33] R. Codina and J. Blasco. A finite element formulation for the Stokes problem allowing equal velocity-pressure interpolation. *Comp. Meth. in Appl. Mech. and Engrg.*, **143**, 373–391 (1997).

[34] R. Codina and J. Blasco. Stabilized finite element method for the transient Navier-Stokes equations based on a pressure gradient projection. *Comp. Meth. in Appl. Mech. and Engrg.*, **182**, 277–300 (2000).

[35] M. Milleli, B. Smith, and D. Lakehal. Some new approaches to bubble plume modeling using CFD. In *Proc. of IMECE'01, 2001 International Mechanical Engineering Congress and Exposition, New York*. ASME, (2001).

[36] U. Piomelli. Large-eddy simulation of turbulent flows. Technical Report TAM Report No. 767, UILU-ENG-94-6023, Theoretical and Applied Mechanics. Univ. Illinois at Urbana-Champaign, (1994).

[37] A. Silva Freire, D. Miranda, L. Luz, and G. Franca. Bubble plumes and the Coanda effect.

*Int. J. Multiphase Flow*, **28**, 1293–1310 (2002).

[38] J. Bendat and A. Piersol. *Random data analysis and measurement procedures*. Wiley series in probability and statistics. John Wiley & Sons, Inc., (2000).

[39] P. Holmes, J. Lumley, and G. Berkooz. *Turbulence, coherent structures, dynamical systems and symmetry*. Cambridge Monographs on Mechanics. Cambridge University Press, (1998).

[40] K. Sene, J. Hunt, and N. Thomas. The role of coherent structures in bubble transport by turbulent shear flow. *J. Fluid Mech.*, **259**, 219–240 (1994).

[41] L. Wang and M. Maxey. Settling velocity and concentration distribution of heavy particles in homogeneous isotropic turbulence. *J. Fluid Mech.*, **256**, 27–68 (1993).